

at  $g = 2.088$  and  $1.831$ . There was no very low-field signal at  $g = 2.088$  seen in the Q-band spectrum. In several spectra, however, a signal at  $g = 1.922$  was observed in the Q-band spectrum.

**Acknowledgment.** The support of the National Science Foundation under Grants NSF-DMR-76-01058 and CHE-77-24964 is gratefully acknowledged by G.D.S. and B.F.F. D.N.H. is grateful for support from National Institutes of Health Grant HL 13652.

**Registry No.** 1, 66172-45-0; 2, 66172-46-1; 3, 66172-47-2; 4, 66172-48-3.

## References and Notes

- School of Chemical Sciences and the Materials Research Laboratory.
- School of Chemical Sciences; Camille and Henry Dreyfus Teacher-Scholar Fellow, 1972-1977; A. P. Sloan Foundation Fellow, 1976-1978.
- B. N. Figgis and G. Robertson, *Nature (London)*, **205**, 694 (1965).
- A. Earnshaw, B. N. Figgis, and J. Lewis, *J. Chem. Soc. A*, 1659 (1966).
- A. P. Ginsberg, R. L. Martin, and R. C. Sherwood, *Inorg. Chem.*, **7**, 932 (1968).
- R. Beckett, R. Colton, B. F. Hoskins, R. L. Martin, and D. G. Vince, *Aust. J. Chem.*, **22**, 2527 (1969).
- A. Hasegawa, *J. Chem. Phys.*, **55**, 3101 (1971).
- (a) G. Kothe, E. Ohmes, J. Brickmann, and H. Zimmermann, *Angew. Chem., Int. Ed. Engl.*, **10**, 938 (1971); (b) J. Brickmann and G. Kothe, *J. Chem. Phys.*, **59**, 2807 (1973).
- (a) A. Hudson and G. R. Luckhurst, *Mol. Phys.*, **13**, 409 (1967); (b) G. Kothe, A. Naujok, and E. Ohmes, *ibid.*, **32**, 1215 (1976).
- G. Kothe, F. A. Neugebauer, and H. Zimmermann, *Angew. Chem., Int. Ed. Engl.*, **11**, 830 (1972).
- B. F. Fieselmann, A. M. McPherson, G. L. McPherson, D. L. Lichtenberger, and G. D. Stucky, for publication in *J. Am. Chem. Soc.* "Beilsteins Handbuch der Organischen Chemie", Vol. 26, p 239.
- P. C. Wailles, R. S. P. Coutts, and H. Weigold, "Organometallic Chemistry of Titanium, Zirconium, and Hafnium", Academic Press, New York, N.Y., 1974, pp 68, 211.
- M. L. H. Green and C. R. Lucas, *J. Chem. Soc., Dalton Trans.*, 1000 (1972).
- R. Jungst, D. Sekutowski, J. Davis, M. Luly, and G. Stucky, *Inorg. Chem.*, **16**, 1645 (1977).
- (a) R. Jungst, D. Sekutowski, and G. Stucky, *J. Am. Chem. Soc.*, **96**, 8108 (1974); (b) D. G. Sekutowski and G. D. Stucky, *Inorg. Chem.*, **14**, 2192 (1975).
- D. G. Sekutowski, Ph.D. Thesis, University of Illinois, 1975.
- L. T. Reynold and G. Wilkinson, *J. Inorg. Nucl. Chem.*, **9**, 88 (1959).
- J. P. Chandler, Program 66, Quantum Chemistry Program Exchange, Indiana University, Bloomington, Ind., 1973.
- D. M. Duggan, E. K. Barefield, and D. N. Hendrickson, *Inorg. Chem.*, **12**, 985 (1973).
- F. E. Mabbs and D. J. Machin, "Magnetism and Transition Metal Complexes", Chapman and Hall, London, 1973, pp 5, 170.
- B. F. Fieselmann, Ph.D. Thesis, University of Illinois, 1977.
- E. I. Lerner and S. J. Lippard, *Inorg. Chem.*, **16**, 1537 (1977).
- S. Emori, M. Inoue, M. Kishita, M. Kubo, S. Mizukami, and M. Kono, *Inorg. Chem.*, **7**, 2418 (1968).
- W. E. Hatfield and F. L. Bunger, *Inorg. Chem.*, **8**, 1194 (1969).
- B. Bleaney and K. D. Bowers, *Proc. R. Soc. London, Ser. A*, **214**, 451 (1952).
- M. F. Lappert and A. R. Sanger, *J. Chem. Soc. A*, 874 (1971).
- K. Issleib and H. Häckert, *Z. Naturforsch., B*, **21**, 519 (1966).
- M. F. Lappert and A. R. Sanger, *J. Chem. Soc. A*, 1314 (1971).
- J. L. Petersen and L. F. Dahl, *J. Am. Chem. Soc.*, **96**, 2248 (1974); **97**, 6422 (1975); J. L. Petersen, D. L. Lichtenberger, R. F. Fenske, and L. F. Dahl, *ibid.*, **97**, 6433 (1975).
- (a) E. Wasserman, L. C. Synder, and W. A. Yager, *J. Chem. Phys.*, **41**, 1763 (1964); (b) J. Reedijk and B. Nieuwenhuijse, *Recl. Trav. Chim. Pays-Bas*, **91**, 533 (1972).
- W. A. Yager, E. Wasserman, and R. M. Cramer, *J. Chem. Phys.*, **37**, 1148 (1962).
- T. R. Felthouse and D. N. Hendrickson, submitted for publication in *Inorg. Chem.*
- B. F. Fieselmann, D. N. Hendrickson, and G. D. Stucky, *Inorg. Chem.*, in press.
- N. D. Chasteen and R. L. Belford, *Inorg. Chem.*, **9**, 169 (1970).
- A. J. McAlees, R. McCrindle, and A. R. Woon-Fat, *Inorg. Chem.*, **15**, 1065 (1976).

Contribution from the School of Chemical Sciences and the Materials Research Laboratory, University of Illinois, Urbana, Illinois 61801

## Magnetic Exchange between Titanium(III) Centers in a Series of Linear Trimetallic Compounds and the Structural Properties of Bis[ $\mu$ -dichloro-bis(cyclopentadienyl)titanium(III)]manganese(II)-Bis(tetrahydrofuran), $[(\eta^5\text{-C}_5\text{H}_5)_2\text{TiCl}]_2\text{MnCl}_2 \cdot 2\text{OC}_4\text{H}_8$

DENNIS SEKUTOWSKI, RUDOLPH JUNGST, and GALEN D. STUCKY\*

Received July 27, 1977

The magnetic properties of a series of  $d^1$  titanium(III) complexes of general formula  $[(\eta^5\text{-C}_5\text{H}_5)_2\text{TiX}]_2\text{MX}_2$  ( $X = \text{halide}$ ,  $M = \text{Zn, Be, Mn}$ ) have been determined. From variable-temperature magnetic susceptibility measurements, an intramolecular antiferromagnetic interaction between the  $d^1$  centers of those compounds containing a diamagnetic ( $d^0$  or  $d^{10}$ ) central metal atom has been observed. The triplet state has been found to be between  $31.4$  and  $13.8 \text{ cm}^{-1}$  above the singlet ground state. Although the magnitude of the exchange coupling constant is larger than one would expect for an intermolecular exchange interaction, it is much lower than what has previously been observed in titanium(III) halide dimers of general formula  $[(\eta^5\text{-C}_5\text{H}_5)_2\text{TiX}]_2$ . Single-crystal X-ray diffraction methods have been employed to determine the molecular structure of  $[(\eta^5\text{-C}_5\text{H}_5)_2\text{TiCl}]_2\text{MnCl}_2 \cdot 2\text{OC}_4\text{H}_8$ . This material crystallizes in the monoclinic space group  $P2_1/c$  ( $C_{2h}^5$ ) with two dimers in a unit cell of dimensions  $a = 8.167$  (5) Å,  $b = 11.453$  (8) Å,  $c = 16.249$  (12) Å, and  $\beta = 91.64$  (3)°. Least-squares refinement of 2768 independent reflections has led to a final weighted  $R$  factor of 0.057. The structure consists of a linear trimetallic molecule with chlorine atoms bridging the metal atoms. The geometry around the central manganese atom is tetragonal as opposed to the pseudotetrahedral geometry of the central atom in the other members of the series. The tetrahydrofuran molecules are coordinated in a trans geometry to the manganese atom and the cyclopentadienyl rings on each titanium atom are eclipsed. Attempts have been made to simulate the magnetic susceptibility of this compound with theoretical equations including both terminal interactions  $\text{Ti}(d^1)\text{-Ti}(d^1)$  and nearest-neighbor interactions  $\text{Ti}(d^1)\text{-Mn}(d^1)$ . The fit was only sensitive to  $J_{1/2,5/2}$  and this was found to be  $-8 \text{ cm}^{-1}$ .

## Introduction

Interest in magnetic interactions has greatly expanded over the last few years. A number of recent reviews have indicated the success that workers in this field have had in correlating the magnitude of the magnetic coupling constant to both structural parameters and molecular orbital calculations for

dimeric metal complexes.<sup>1-3</sup> The results have been particularly useful in the understanding of exchange mechanisms. However, very few studies have been undertaken to examine the magnetic properties of trimetallic systems.

Three metals can be geometrically arranged in a triangular or linear configuration. Magnetic exchange in homonuclear

compounds where all the metal atoms are located on the corners of an equilateral triangle around an oxygen atom have been determined for  $[\text{Cr}_3\text{O}(\text{Oac})_6(\text{H}_2\text{O})_3]\text{Cl}\cdot 6\text{H}_2\text{O}$  ( $d^3-d^3-d^3$ ) and  $[\text{Fe}_3\text{O}(\text{Oac})_6(\text{H}_2\text{O})_3]\text{Cl}\cdot 6\text{H}_2\text{O}$  ( $d^5-d^5-d^5$ ).<sup>4-7</sup> The compounds were found to have an antiferromagnetic interaction with  $J = -10.4 \text{ cm}^{-1}$  and  $J = -30 \text{ cm}^{-1}$ , respectively. Variable-temperature magnetic susceptibility measurements on trimeric iron(III) alkoxides have also indicated an antiferromagnetic interaction between the metal centers, and the results are consistent with the metal atoms being in an equilateral triangle; however structural data are lacking.<sup>8</sup> Sinn has reported the magnetic properties of a number of trimetallic complexes where the metal atoms are in an isosceles triangle arrangement.<sup>9</sup> Two copper atoms ( $d^9$ ) were bridged by a variety of paramagnetic and diamagnetic metal centers; however a measurable value for exchange interactions between the terminal metals was not found. Since the magnetic data were only collected down to liquid nitrogen temperatures, the possibility of such an interaction cannot be excluded for these compounds. The only example of 1,3 magnetic exchange within a linear triad of metal atoms has been found by Ginsberg for  $\text{Ni}_3(\text{acac})_6$ . Variable-temperature magnetic susceptibility studies have shown that an antiferromagnetic exchange between the terminal nickel atoms via the paramagnetic nickel(II) central atom does yield an improved fit to the experimental data.<sup>10,11</sup> Studies have not been undertaken for linear trimetallic complexes where the central metal is diamagnetic.

The limited number of magnetic studies of trimetallic systems is probably a result of the synthetic difficulties involved in preparing a series of such complexes in which one can introduce a systematic variation in geometry in order to observe its influence on the magnetic coupling constant. With the exception of the compounds reported in this paper, all linear trimetallic organometallic complexes that have been structurally characterized to date have been diamagnetic.

We have previously communicated our discovery of antiferromagnetic exchange between Ti(III) centers via a diamagnetic metal center in a series of nearly linear trimetallic complexes.<sup>12</sup> We wish now to report the details and interpretation of our magnetic data for these systems and the results of exchange through a paramagnetic center in  $[(\eta^5\text{-C}_5\text{H}_5)_2\text{TiCl}]_2\text{MnCl}_2\cdot 2\text{OC}_4\text{H}_8$ . The physical properties of this latter compound indicated that it was not isostructural with the other members of the series, and a three-dimensional X-ray analysis of the material was undertaken to ascertain its molecular structure.

## Experimental Section

**Synthesis.** The compounds were all prepared and characterized as given in ref 13.

**X-ray Data.** Preliminary precession photographs of  $[(\eta^5\text{-C}_5\text{H}_5)_2\text{TiCl}]_2\text{MnCl}_2\cdot 2\text{OC}_4\text{H}_8$  (Mo  $K\alpha$  radiation) revealed that the crystals were monoclinic. The observed systematic absences  $h0l$ ,  $l = 2n + 1$ , and  $0k0$ ,  $k = 2n + 1$ , are compatible with space group  $P2_1/c$  ( $C_{2h}^2$ ; No. 14). A triangular prism with edges which varied from 0.07 to 0.13 mm was used for data collection.

Lattice parameters were obtained by a least-squares refinement of 14 reflections, which were carefully hand centered on a Picker four-circle diffractometer ( $T = 23^\circ\text{C}$ ,  $\lambda = 0.71069 \text{ \AA}$ ). The final values obtained were  $a = 8.167(5) \text{ \AA}$ ,  $b = 11.453(8) \text{ \AA}$ ,  $c = 16.249(12) \text{ \AA}$ , and  $\beta = 91.64(3)^\circ$ . The density calculated on the basis of two molecules per unit cell is  $1.523 \text{ g cm}^{-3}$ , while the observed value of  $1.53 \pm 0.03 \text{ g cm}^{-3}$  was obtained by flotation in a bromobenzene and *m*-bromoaniline mixture. Several  $\omega$  scans showed a typical peak width at half-height to be  $0.125^\circ$  indicating that the mosaicity was acceptable for data collection.

Intensity data were measured on a fully automated Picker four-circle diffractometer using Mo  $K\alpha$  radiation monochromated by a highly oriented graphite crystal. A  $\theta$ - $2\theta$  scan technique was used with a scan width of  $1.5^\circ$ , a scan rate of  $2^\circ/\text{min}$ , and a takeoff angle of  $1.6^\circ$ .

**Table I.** Positional Parameters for the Nonhydrogen Atoms in  $[(\eta^5\text{-C}_5\text{H}_5)_2\text{TiCl}]_2\text{MnCl}_2\cdot 2\text{OC}_4\text{H}_8$

Atoms	x	y	z
Mn	0.000	0.000	0.0000
Ti	-0.25715 (11)	0.18938 (8)	0.14336 (5)
Cl(1)	-0.27867 (14)	0.09708 (11)	-0.00081 (11)
Cl(2)	0.2594 (15)	0.8991 (11)	0.1428 (7)
C(1)	-0.3391 (9)	0.00961 (5)	0.1986 (5)
C(2)	-0.4810 (9)	0.0630 (7)	0.1669 (4)
C(3)	-0.5085 (8)	0.1608 (7)	0.2123 (5)
C(4)	-0.3874 (10)	0.1699 (6)	0.2719 (4)
C(5)	-0.2832 (8)	0.0780 (7)	0.2650 (4)
C(6)	-0.1284 (8)	0.3434 (5)	0.0769 (4)
C(7)	-0.2966 (10)	0.3593 (5)	0.0630 (4)
C(8)	-0.3612 (8)	0.3843 (6)	0.1383 (6)
C(9)	-0.2366 (12)	0.3837 (6)	0.1967 (4)
C(10)	-0.0935 (8)	0.3577 (5)	0.1602 (4)
O	0.1124 (4)	0.3390 (3)	0.4495 (2)
C(11)	0.2610 (7)	0.2855 (5)	0.4797 (3)
C(12)	0.2823 (9)	0.1789 (6)	0.4325 (4)
C(13)	0.1495 (9)	0.1702 (7)	0.3721 (5)
C(14)	0.0451 (7)	0.2741 (5)	0.3807 (3)

Background counts, each of 10-s duration, were taken at both ends of the scan. Copper foil attenuators were automatically inserted in front of the counter whenever the counting rate exceeded 10000 counts/s. Three standards were measured every 50 reflections in order to check for crystal and counter stability. Whenever these standards showed any significant fluctuations during data collection, the crystal was recentered and that particular section of data was recollected. One quadrant of intensity data ( $hkl$  and  $h\bar{k}l$ ) was measured to  $50^\circ$  in  $2\theta$ . A total of 2768 unique reflections were measured, 1510 of which were considered observed by the criteria  $I_{\text{obsd}} > 3\sigma_c(I)$ . Here  $\sigma_c = [T_c + 0.25(t_c/t_b)^2(B_1 + B_2)]^{1/2}$  where  $T_c$  is the total counts,  $t_c/t_b$  is the ratio of the time counting peak intensity to that spent counting backgrounds, and  $B_1$  and  $B_2$  are the background counts. Initial structure solution was accomplished using just the observed reflections.

Final refinement using all of the data was carried out with weights assigned on the basis of counting statistics. No significant systematic variation of  $w(F_o - F_c)^2$  was observed with respect to  $(\sin \theta)/\lambda$  or the magnitude of the structure factors. The nonhydrogen scattering factors were taken from the tabulation of Cromer and Waber<sup>14</sup> and the hydrogen scattering factors from Stewart, et al.<sup>15</sup> Anomalous dispersion corrections for the titanium, manganese and chlorine atoms were those of Cromer and Liberman.<sup>16</sup> Lorentz and polarization corrections and the calculation of the observed structure factor amplitudes from the raw data were carried out using the program VANDY. Absorption corrections were made ( $\mu = 13.3 \text{ cm}^{-1}$ ) with the program ORABS.

**Structure Determination and Refinement.** The structure was solved in a straightforward manner by application of direct-methods (FAME and MULTAN) and Fourier techniques. All computer programs employed have been previously referenced.<sup>17</sup> From the generated  $E$  map the titanium and manganese atom positions were found, and they coincided with the positions obtained from a Patterson map. From density measurements, only half of the molecule could be in an asymmetric unit of the cell, indicating that the central manganese atom was on the crystallographic center of inversion. This was consistent with the metal atom positions, and subsequent application of Fourier calculations and least-squares refinement led to the discovery of all nonhydrogen atoms.

Final anisotropic refinement of all parameters with the exception of the hydrogen atom temperature factors, which were set equal to the isotropic temperature factor of the carbon atom to which they were bonded, gave an error of fit equal to 1.4275 and  $R_1 = \sum |F_o| - |F_c| / \sum |F_o| = 0.095$  and  $R_2 = [\sum w(|F_o| - |F_c|)^2 / \sum wF_o^2]^{1/2} = 0.057$ .

Final positional parameters, anisotropic thermal parameters, interatomic distances, and bond angles are given in Tables I-IV, respectively.

**Physical Measurements.** Variable-temperature (4.2-295 K) magnetic susceptibility measurements were made with a Princeton Applied Research Model 150A vibrating-sample magnetometer calibrated with  $\text{CuSO}_4\cdot 5\text{H}_2\text{O}$ . A calibrated gallium arsenide diode was used in the temperature-controlling and -sensing device. All experimental data were corrected for diamagnetism using Pascal's constants and computer fit to theoretical expressions with STEPT by

Table II. Anisotropic Thermal Parameters for the Nonhydrogen Atoms in  $[(C_5H_5)_2TiCl]_2MnCl_2 \cdot 2OC_4H_8$ 

Atom	$U_{11}^a$	$U_{22}$	$U_{33}$	$U_{12}$	$U_{13}$	$U_{23}$
Mn	0.0391 (6)	0.04087 (6)	0.0413 (5)	0.0007 (5)	-0.0007 (5)	0.0006 (5)
Ti	0.0420 (5)	0.0467 (6)	0.0456 (5)	0.0020 (5)	0.0062 (4)	-0.0046 (5)
Cl(1)	0.0377 (7)	0.0542 (8)	0.0485 (8)	0.0025 (6)	-0.0056 (5)	-0.0058 (7)
Cl(2)	0.0428 (7)	0.0593 (9)	0.0425 (7)	0.0012 (7)	-0.0030 (5)	0.0041 (7)
C(1)	0.097 (5)	0.051 (4)	0.100 (5)	0.010 (4)	0.050 (5)	0.008 (4)
C(2)	0.074 (5)	0.116 (6)	0.063 (4)	0.046 (5)	0.002 (3)	0.013 (5)
C(3)	0.050 (4)	0.105 (6)	0.102 (5)	0.006 (4)	0.028 (4)	0.020 (5)
C(4)	0.096 (5)	0.088 (5)	0.057 (4)	0.028 (4)	0.028 (4)	0.019 (4)
C(5)	0.065 (4)	0.107 (6)	0.063 (4)	0.011 (4)	0.006 (3)	0.029 (4)
C(6)	0.091 (5)	0.049 (3)	0.063 (4)	0.004 (3)	0.028 (3)	0.002 (3)
C(7)	0.107 (6)	0.051 (4)	0.083 (5)	0.004 (4)	0.036 (5)	0.005 (4)
C(8)	0.069 (5)	0.058 (4)	0.138 (7)	0.016 (4)	0.034 (5)	0.004 (5)
C(9)	0.155 (8)	0.052 (4)	0.078 (5)	0.004 (5)	0.025 (5)	-0.015 (4)
C(10)	0.077 (5)	0.058 (4)	0.083 (5)	0.017 (3)	0.017 (4)	-0.010 (4)
O	0.048 (2)	0.058 (2)	0.049 (3)	0.009 (2)	0.007 (1)	-0.011 (2)
C(11)	0.053 (3)	0.062 (4)	0.069 (4)	0.013 (3)	0.007 (3)	-0.011 (3)
C(12)	0.096 (5)	0.097 (5)	0.107 (5)	0.038 (5)	0.013 (5)	-0.041 (5)
C(13)	0.097 (1)	0.112 (6)	0.120 (7)	0.019 (5)	-0.013 (5)	-0.064 (6)
C(14)	0.078 (4)	0.069 (4)	0.043 (3)	-0.002 (3)	-0.005 (3)	-0.008 (3)

<sup>a</sup> The form of the anisotropic ellipsoid is  $\exp[-2\pi^2(h^2U_{11}a^{*2} + k^2U_{22}b^{*2} + l^2U_{33}c^{*2} + 2hkU_{12}a^*b^* + 2hlU_{13}a^*c^* + 2klU_{23}b^*c^*)]$ .

Table III. Interatomic Distances (Å) for the Nonhydrogen Atoms in  $[(C_5H_5)_2TiCl]_2MnCl_2 \cdot 2OC_4H_8$ <sup>a</sup>

Mn-Cl(1)	2.533 (2)	Ti-C(2)	2.367 (6)
Mn-Cl(2)	2.531 (2)	Ti-C(3)	2.389 (6)
Mn-O	2.227 (3)	Ti-C(4)	2.382 (6)
Mn-Ti	3.850 (2)	Ti-C(5)	2.367 (6)
Ti-Cl(1)	2.572 (2)	Ti-C(6)	2.334 (6)
Ti-Cl(2)	2.578 (2)	Ti-C(7)	2.360 (6)
Cl(1)-Cl(2)	3.355 (3)	Ti-C(8)	2.390 (6)
Cl(1)-Cl(2)'	3.793 (3)	Ti-C(9)	2.392 (7)
Ti-C(1)	2.351 (6)	Ti-C(10)	2.357 (6)
Cp 1			
C(1)-C(2)	1.396 (9)	C(4)-C(5)	1.360 (9)
C(2)-C(3)	1.363 (9)	C(5)-C(1)	1.400 (9)
C(3)-C(4)	1.369 (9)		
Cp 2			
C(6)-C(7)	1.397 (9)	C(9)-C(10)	1.359 (9)
C(7)-C(8)	1.377 (9)	C(10)-C(6)	1.386 (8)
C(8)-C(9)	1.371 (10)		
THF			
O-C(11)	1.434 (6)	C(13)-C(14)	1.472 (9)
C(11)-C(12)	1.455 (8)	C(14)-O	1.438 (6)
C(12)-C(13)	1.446 (9)		

<sup>a</sup> Errors in the lattice parameters are included in the estimated standard deviations.

Table IV. Bond Angles (deg) for the Nonhydrogen Atoms in  $[(C_5H_5)_2TiCl]_2MnCl_2 \cdot 2OC_4H_8$ 

Cl(2)-Mn-Cl(1)	82.99 (5)	O-Mn-Cl(1)	90.8 (1)
Cl(2)-Mn-Cl(1)'	97.01 (5)	O-Mn-Cl(2)	88.6 (1)
Cl(1)-Ti-Cl(2)	81.31 (6)	O-Mn-Cl(1)'	89.2 (1)
Mn-Cl(1)-Ti	97.91 (5)	O-Mn-Cl(2)'	91.4 (1)
Mn-Cl(2)-Ti	97.78 (5)		
THF			
C(11)-O-C(14)	110.2 (4)	C(12)-C(13)-C(14)	107.8 (5)
O-C(11)-C(12)	106.9 (5)	C(13)-C(14)-O	106.4 (5)
C(11)-C(12)-C(13)	108.4 (6)		
Cp 1			
C(2)-C(1)-C(5)	106.7 (6)	C(5)-C(4)-C(3)	108.9 (6)
C(3)-C(2)-C(1)	108.0 (6)	C(1)-C(5)-C(4)	107.8 (6)
C(4)-C(3)-C(2)	108.6 (6)		
Cp 2			
C(7)-C(6)-C(10)	108.4 (6)	C(10)-C(9)-C(8)	109.3 (6)
C(8)-C(7)-C(6)	106.5 (6)	C(6)-C(10)-C(9)	107.3 (6)
C(9)-C(8)-C(7)	108.5 (6)		

J. P. Chandler, Indiana University. The absolute accuracy of molar susceptibilities measured on this apparatus is believed to approach  $\pm 2\%$ .

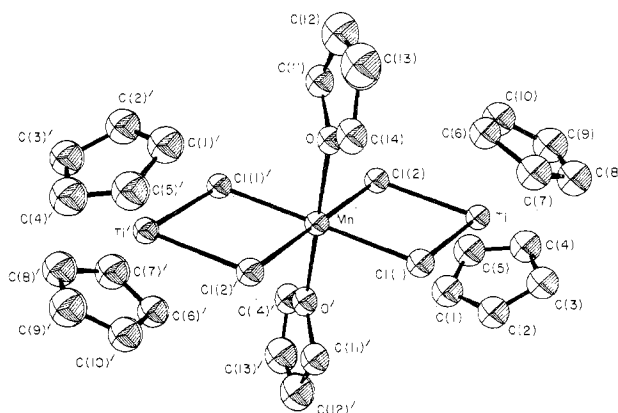


Figure 1. Molecular structure of  $[(C_5H_5)_2TiCl]_2MnCl_2 \cdot 2OC_4H_8$ . Thermal ellipsoids are shown at the 42% probability level.

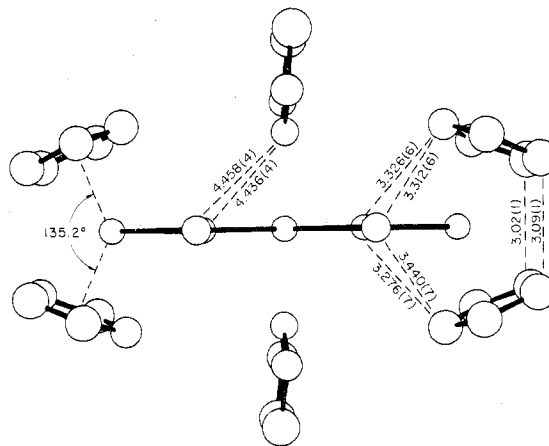


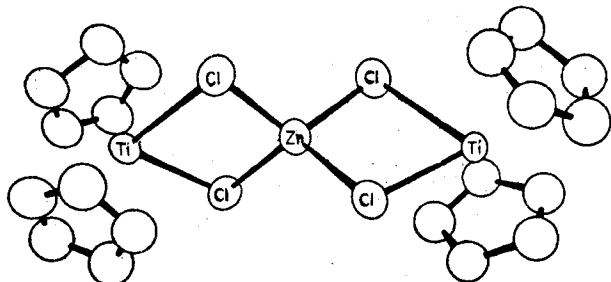
Figure 2. Perspective view of  $[(C_5H_5)_2TiCl]_2MnCl_2 \cdot 2OC_4H_8$  looking down the plane containing the heavy atoms. Interatomic distances are given in angstroms.

Q-Band EPR data were obtained on a Varian WL-115 spectrometer equipped with a 12-in. magnet capable of fields up to 25 kG and an E-110 microwave bridge. A Vacuum Atm., Inc., drybox was employed for storing and loading of samples into X-ray and EPR capillaries and magnetic susceptibility cells.

## Discussion

**Structural Properties.** The molecular structure of  $[(\eta^5-C_5H_5)_2TiCl]_2MnCl_2 \cdot 2OC_4H_8$  is shown in Figures 1 and 2. The central manganese atom lies on a crystallographic in-

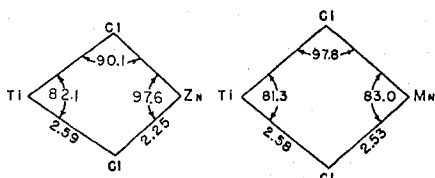
version center. The metal atoms are collinear (Ti–Mn–Ti = 180°) and are bridged by chlorine atoms. Figure 2 clearly shows that all of the heavy atoms (Ti, Mn, Cl) lie in a plane even though this is not imposed by  $C_i$  ( $\bar{1}$ ) symmetry. The trans coordination of the tetrahydrofuran molecules to the manganese atom yields a tetragonal geometry around the central metal ( $D_{2h}$  for the molecule). This result is in contrast to the other members of the chemical series discussed in this paper, which have a pseudotetrahedral arrangement around the central metal, as has been observed from X-ray data for  $[(\eta^5\text{-C}_5\text{H}_5)_2\text{TiCl}]_2\text{ZnCl}_2\cdot\text{C}_6\text{H}_6$ .<sup>13</sup> In this compound the



Ti–Zn–Ti angle was found to be 173.4 (1)° with a Ti–Ti intramolecular distance of 6.828 (4) Å compared to 7.700 (2) Å in the manganese compound.

The manganese structure is symmetric with respect to the distance of the two chlorine atoms to a particular metal atom, e.g., Mn–Cl(1) and Mn–Cl(2) are 2.533 (2) and 2.531 (2) Å, respectively, and Ti–Cl(1) and Ti–Cl(2) are 2.572 (2) and 2.578 (2) Å, respectively. The Mn–Cl distances are on the order of other Mn–Cl distances that have been observed for the hydrated salts of tetrachloromanganate(II) of general formula  $\text{M}_2\text{MnCl}_4\cdot 2\text{H}_2\text{O}$  (M = K, Rb, Cs) which contain pseudooctahedral geometry around the manganese atom and Mn–Cl distances between 2.53 and 2.58 Å.<sup>19</sup> The Mn–O distance is however longer for tetrahydrofuran (2.227 (2) Å) than for the coordinated water molecules (between 2.08 and 2.175 Å) within these hydrates.

A comparison of the chlorine bridging geometries between the zinc and manganese complexes does not show any unusual differences. The Ti–Cl distances are the same to within 3 times the standard deviations. The angle around the central metal atom Cl–M–Cl varies from 97.6° around zinc to 83.0° around manganese. While a decrease is expected since the manganese atom is six-coordinate and the zinc atom is four-coordinate, the distance of 3.793 (3) Å between Cl(1) and Cl(2)' is too large for any significant steric effect between the chlorine atoms in the  $\text{MnCl}_4$  plane. The reduction of the  $\text{MCl}_2$  angle causes other variations between the ring systems, as shown here. The  $\text{TiCl}_2$  angle is reduced by almost 1° and the



bridgehead angle is opened from 90.1 to 97.8°. This increase in the bridgehead angle is also accompanied by a decrease in the bridgehead Cl–Cl distance from 3.387 (2) to 3.355 (3) Å.

The Ti–Mn distance of 3.850 (2) Å is well outside the range expected for consideration of metal–metal bonding. From a structural viewpoint the molecule appears to be a  $d^1$ – $d^5$ – $d^1$  system.

The cyclopentadienyl ring centroid–Ti–ring centroid angle of 135.2° is within the range (129–138.6°) observed for other bis(cyclopentadienyl)titanium compounds.<sup>17</sup> The Ti–ring centroid distance was found to be 2.06 Å. The cyclo-

pentadienyl rings are eclipsed, and the thermal motion of the individual ring carbon atoms is low. The highest thermal parameters observed are for the  $\beta$ -carbon atoms of the tetrahydrofuran molecule. The closest contact between cyclopentadienyl rings is shown in Figure 2, indicating the lack of any sort of steric interactions. The C–C distances within the rings vary from 1.400 (9) to 1.359 (9) Å, and the largest deviation of a carbon atom from the best plane calculated for the cyclopentadienyl rings is only 0.005 (6) Å.

**Magnetic Exchange.** The interaction between spin centers can be represented by the spin Hamiltonian

$$\mathcal{H} = -2 \sum_{i>j}^n J_{ij} S_i \cdot S_j$$

where  $J_{ij}$  is the exchange integral between the  $i$ th and  $j$ th centers. The magnetism of two coupled titanium(III)  $d^1$  centers ( $s_1 = s_2 = 1/2$ ) can be expressed by the Bleaney–Bowers equation

$$\chi_M = \frac{2g^2\beta^2N}{3k(T-\Theta)} [1 + 1/3 \exp(-2J/kT)]^{-1} + N\alpha$$

where  $-2J$  corresponds to the singlet–triplet energy separation and  $N\alpha$  is the temperature-independent paramagnetism. In our studies the TIP was set at  $260 \times 10^{-6}$  per trimetallic molecule and values for  $J$ ,  $g$ , and  $\Theta$  were obtained by a least-squares fit of the data to the above equation for the compounds containing a central metal of spin equal to zero.

If the central metal has a spin not equal to zero, then the possibility of terminal and nearest-neighbor interactions exists. Sinn<sup>9,18</sup> has derived an equation to represent the magnetism in such cases, and because of previous misprints it is given below for the case where the terminal centers each have spin of  $1/2$  ( $s_1 = s_2 = 1/2$ )

$$\chi_M = \frac{g^2\beta^2N}{k(T-\Theta)} (A/B) + N\alpha$$

where

$$A = \sum_{i=1}^{2S_M-1} (S_M - i)^2 \exp\left[\frac{-(2S_M + 2)J_{1/2, S_M}}{kT}\right] + \sum_{i=1}^{2S_M+1} (S_M - i + 1)^2 \exp(-2J_{1/2, S_M}/kT) + \sum_{i=1}^{2S_M+1} (S_M - i + 1)^2 \exp(-2J_{1/2, 1/2}/kT) + \sum_{i=1}^{2S_M+3} (S_M - i + 2)^2 \exp(2S_M J_{1/2, S_M}/kT)$$

and

$$B = (2S_M - 1) \exp[-(2S_M + 2)J_{1/2, S_M}/kT] + (2S_M + 1) \exp(-2J_{1/2, S_M}/kT) + (2S_M + 1) \exp(-2J_{1/2, 1/2}/kT) + (2S_M + 3) \exp(2S_M J_{1/2, S_M}/kT)$$

$S_M$  is the spin of the central metal ( $S_M = 5/2$  for the manganese compound),  $J_{1/2, 1/2}$  is the coupling constant for interaction between the spin  $1/2$  metals, and  $J_{1/2, S_M}$  is the coupling constant for interaction between the terminal spin  $1/2$  metal and the central metal atom.

**Magnetic Susceptibility of Compounds with a Diamagnetic Central Metal.** Before discussion of the magnetic results, a

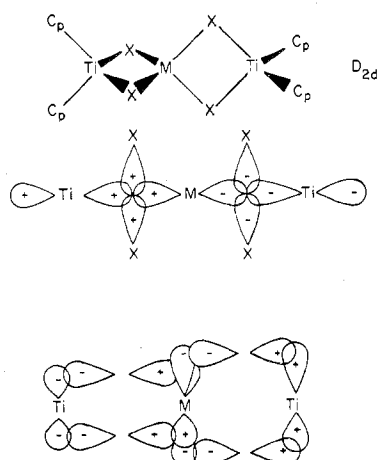


Figure 3. Possible exchange mechanisms for titanium(III) trimetallic complexes with a tetrahedrally coordinated central metal.

Table V. Percent Orbital Character ( $a_1$  Symmetry)

	M			Cl		Cp	
	$d_{z^2}$	$d_{x^2-y^2}$	$p_x$	$p_z$	$a_2$	$e_1$	$e_2$
$(\eta^5\text{-C}_5\text{H}_5)_2\text{TiCl}_2$	69.5	4.9	0.9	16.1	0.3	0.4	6.1 (LUMO)
$(\eta^5\text{-C}_5\text{H}_5)_2\text{VCl}_2$	67.6	3.3	0.8	22.3	0.2	0.3	4.4 (HOMO)

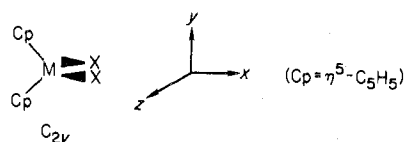


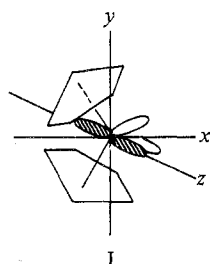
Figure 4. Temperature dependence of the magnetic susceptibility and effective moment per titanium ( $\mu_B$ ) for  $[(\text{C}_5\text{H}_5)_2\text{TiCl}]_2\text{BeCl}_2 \cdot 2\text{C}_6\text{H}_6$ .

Table VI. Best-Fit Parameters for Magnetic Data<sup>a</sup>

Compd	$J$ , $\text{cm}^{-1}$	$g$	$\Theta$ , K
$[(\eta^5\text{-C}_5\text{H}_5)_2\text{TiCl}]_2\text{ZnCl}_2 \cdot 2\text{C}_6\text{H}_6$	-8.9	2.01	0.49
$[(\eta^5\text{-C}_5\text{H}_5)_2\text{TiBr}]_2\text{ZnBr}_2 \cdot 2\text{C}_6\text{H}_6$	-15.7	1.94	-1.37
$[(\eta^5\text{-C}_5\text{H}_5)_2\text{TiCl}]_2\text{BeCl}_2 \cdot 2\text{C}_6\text{H}_6$	-6.9	1.91	1.87
$[(\eta^5\text{-CH}_2\text{C}_5\text{H}_4)_2\text{TiCl}]_2\text{ZnCl}_2$	-7.3	1.92	0.69
$[(\text{CH}_3)_2\text{Si}(\eta^1, \eta^5\text{-C}_5\text{H}_4)_2\text{TiCl}]_2\text{ZnCl}_2$	-6.9	1.90	0.77

<sup>a</sup> TIP was taken as  $260 \times 10^{-6}/\text{mol}$  for all compounds.

few comments about the electronic structure of bis(cyclopentadienyl)titanium complexes and its relevance to magnetic exchange mechanisms will be given. A number of theories have been proposed to explain the bonding in bis(cyclopentadienyl) systems.<sup>20-23</sup> In the most favored model for 18-electron systems of general formula  $(\eta^5\text{-C}_5\text{H}_5)_2\text{ML}_2$ , the "lone pair" of electrons are predominantly in an orbital which lies in the L-M-L plane but is normal to the twofold axis of the molecule, as shown in I.



Recently Dahl and co-workers<sup>24-27</sup> have performed non-parameterized Fenske-Hall molecular orbital calculations upon  $(\eta^5\text{-C}_5\text{H}_5)_2\text{MCl}_2$  where  $M = \text{Ti}$  and  $\text{V}$ . They have verified their theoretical calculations experimentally by photoelectron spectroscopy and single-crystal electron paramagnetic resonance studies. The unpaired electron in the  $d^1$  system  $(\eta^5\text{-C}_5\text{H}_5)_2\text{VCl}_2$  is primarily in a molecular orbital of  $a_1$  symmetry which is 3-5 eV below the lowest unoccupied molecular orbital. As shown in Table V the unpaired electron density is in a  $d$  orbital primarily  $d_{z^2}$  in character. Although this is compatible with the model described (I), the  $a_1$  molecular orbital does contain some  $d_{x^2-y^2}$  character. The analysis should also apply to the isoelectronic  $[(\eta^5\text{-C}_5\text{H}_5)_2\text{TiCl}_2]^-$  fragment.

The mechanism of antiferromagnetic exchange is generally accepted to involve the mutual pairing of electron spin by some form of orbital overlap. Knowing the geometry and electronic state of the trimetallic molecules containing a diamagnetic

central metal, we can postulate a number of possible exchange pathways. Two pathways which are consistent with the symmetry of the molecule are illustrated in Figure 3. The upper pathway is a direct mechanism in which a  $d$  orbital could be used rather than a  $p$  orbital of the central metal as shown. The participation of ligand orbitals is not necessary in this type of interaction. The combination at the bottom of the figure is a superexchange path which involves the more highly populated  $\text{Ti } d_{z^2}$  orbital. This type of mechanism is only possible if an  $s$  or  $d$  orbital is available on the central metal.

In order to obtain an estimate of the intermolecular exchange interaction that one might expect for cyclopentadienyl  $d^1$  systems, the magnetic susceptibility of  $(\eta^5\text{-C}_5\text{H}_5)_2\text{VCl}_2$  and  $[(\eta^5\text{-C}_5\text{H}_5)_2\text{Ti} \cdot \text{DME}]_2\text{Zn}_2\text{Cl}_6$  were measured. A small interaction was found at low temperatures for  $(\eta^5\text{-C}_5\text{H}_5)_2\text{VCl}_2$ ; however no maximum was observed in the susceptibility curve. Use of the dimer model estimates an absolute magnitude for the coupling constant of less than  $2 \text{ cm}^{-1}$ . The dimethoxyethane (DME) complex has been shown crystallographically<sup>13</sup> to contain isolated  $\text{Ti(III)}$  monomeric cations, and the very slight decrease in effective moment per  $\text{Ti}$  at low temperatures can be simulated by a dimer  $J$  smaller than  $-1 \text{ cm}^{-1}$ .

Since the magnitude of the exchange integral that is observed in the trimetallic compounds is considerably larger than these limiting values for an intermolecular exchange between  $\text{Ti(III)}$  centers, we can interpret this as evidence that an intramolecular mechanism must be operative within these molecules. Examination of the packing in  $[(\eta^5\text{-C}_5\text{H}_5)_2\text{TiCl}]_2\text{ZnCl}_2 \cdot 2\text{C}_6\text{H}_6$  does not reveal interactions between molecules that would suggest any source of intermolecular exchange. Exchange coupling via the benzene molecules is also excluded since two of the compounds crystallize without solvent molecules in the crystal lattice and still show a magnetic interaction of the same magnitude.

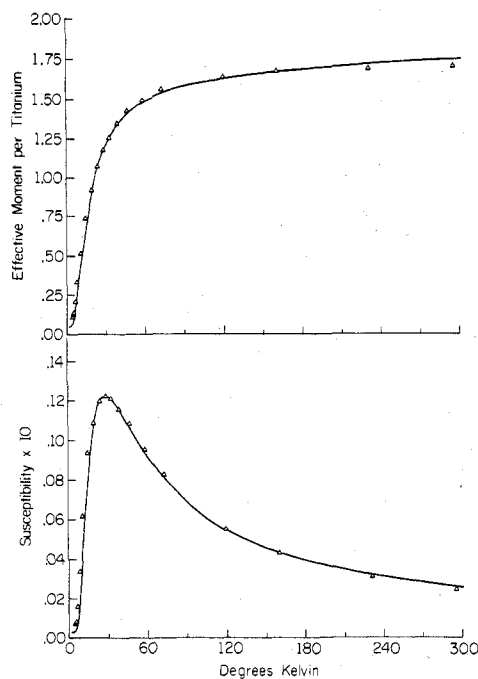


Figure 5. Temperature dependence of the magnetic susceptibility and effective moment ( $\mu_B$ ) per titanium for  $[(C_5H_5)_2TiBr]_2ZnBr_2 \cdot 2C_6H_6$ .

Table VI lists the magnetic parameters obtained for the trimetallic systems which have been successfully synthesized to date. In all cases a very well defined maximum in the susceptibility vs. temperature curves was observed. Representative graphs are given in Figures 4 and 5. The observed and calculated magnetic data (Tables VII–XII) are given as supplementary material. The low values of the experimental magnetic susceptibility at liquid helium temperatures are a good indication of the purity of the samples, since paramagnetic impurities will cause this value to increase. Because fits of the magnetic data give reasonable  $g$  values, attempts to use  $g$  values determined by ESR analysis have not been made. The ESR  $g$  values are within 0.1 of those derived from magnetic data simulation.

In the zinc chloride complexes it appears that neither substitution of a methyl group onto the cyclopentadienyl ring nor perturbation of the Cp–Ti–Cp angle by tying the cyclopentadienyl rings together with a dimethylsilyl group has influenced the coupling constant to any large extent. This result is in contrast to the  $(\eta^5-C_5H_5)_2TiCl$  dimer system where methyl substitution onto the cyclopentadienyl ring causes the coupling constant to increase from  $J = -111 \text{ cm}^{-1}$  to  $J = -160 \text{ cm}^{-1}$ .<sup>28</sup> This phenomenon, however, can be easily explained if one assumes that direct metal–metal exchange plays a significant role in the  $[(\eta^5-C_5H_5)_2TiCl]_2$  dimer complexes. A small change in the metal–metal distance will cause acute differences in the overlap integral and respectively in the coupling constant. The Ti–Ti distance is shorter in the methyl ring substituted complex than in the unsubstituted complex, in agreement with the stronger coupling observed in the former. In the  $[(\eta^5-C_5H_5)_2TiBr]_2$  dimer complexes, where the Ti–Ti distance has been shown to be over 0.15 Å larger, direct metal–metal interactions should play a substantially less important role than in the chloride dimers. Methyl substitution in the cyclopentadienyl ring of the bromide complex has been shown not to influence the coupling constant in this system. Likewise, in the trimetallic complexes direct Ti–Ti interactions cannot be important since the titanium atoms are over 6 Å apart.

Switching the central metal from zinc to beryllium also has not drastically changed the singlet–triplet energy separation

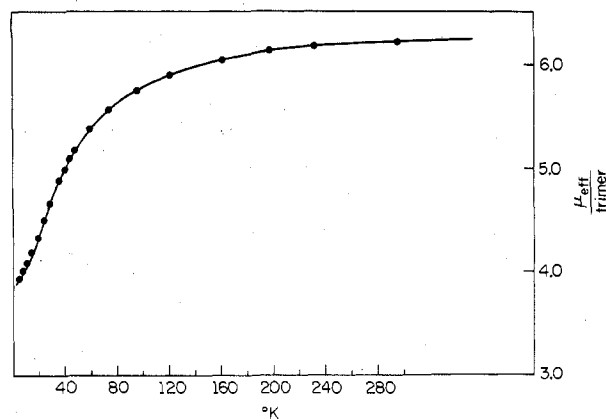


Figure 6. Temperature dependence of the experimental effective moment ( $\mu_B$ ) per trimetallic molecule of  $[(C_5H_5)_2TiCl]_2MnCl_2 \cdot 2OC_4H_8$ . Diamagnetic correction of  $-416 \times 10^{-6}$  cgsu was applied.

of these systems. The beryllium compound shows that  $d$  orbitals are *not* a requirement of the central metal atom in order to have exchange.

The largest effect observed in the magnetic data is due to a change of the bridging halide atoms. This effect would be consistent with a superexchange mechanism. Martin has pointed out that for a superexchange mechanism, the transfer integral and hence the exchange coupling should become larger as the electronegativity of the anion decreases.<sup>29</sup> The magnitude of  $J$  should therefore be  $Br > Cl$  if a superexchange mechanism predominates. Since the coupling becomes stronger on replacement of chlorine by bromine atom bridges, a superexchange mechanism appears likely. If only a direct mechanism was operative, the opposite effect would be expected; i.e., the absolute value of the coupling constant should decrease since the Ti–Zn distance is expected to be longer in the bromide-bridged compound, hence reducing the direct overlap of metal orbitals.

**Magnetic Susceptibility of a Ti–Mn–Ti Complex.** The compound  $[(\eta^5-C_5H_5)_2TiCl]_2MnCl_2 \cdot 2OC_4H_8$  is more difficult to treat theoretically because of the large number of unpaired electrons. The temperature dependence of the effective moment is given in Figure 6. The room-temperature moment of  $6.24 \mu_B$  is under the spin-only value of  $7.94 \mu_B$  for seven unpaired electrons. This value was checked by remeasuring the magnetic susceptibility at room temperature on a torsion balance, and the value of  $6.22 \mu_B$  obtained is within experimental error of the previous value. A low room-temperature moment is not surprising in electron-rich systems. One can represent the spin state as  $(S, S')$  where  $S$  is the total spin state and  $S'$  is the spin state obtained by coupling only the terminal paramagnetic centers. An energy diagram for such a system has been calculated.<sup>9</sup> The  $(7/2, 1)$  state is 12J above the ground state. The energy of this state is high enough so that it is not fully populated at room temperature, and many molecules are in the  $(5/2, 1)$  or  $(5/2, 0)$  states. Since the magnetic moment is a bulk quantity, a lower moment is therefore obtained. Sinn<sup>9</sup> has noticed the same effect in other trimetallic compounds.

The value of  $\mu_{\text{eff}}$  at 4.2 K is  $3.93 \mu_B$  per molecule (Figure 6) which is close to the value  $3.87 \mu_B$  predicted for three unpaired electrons from the spin-only formula. This implies that the coupling between the titanium and the manganese is antiferromagnetic ( $J_{1/2,5/2}$  is negative).

In fitting the data to the theoretical equation, an attempt was made to determine both of the interaction parameters  $J_{1/2,5/2}$  and  $J_{1/2,1/2}$ , but this proved to be difficult with manganese as the central metal atom. Figure 7 shows the theoretical curves for several sets of parameters, the best-fit values being  $J_{1/2,5/2} = -8.24 \text{ cm}^{-1}$ ,  $J_{1/2,1/2} = -8.1 \text{ cm}^{-1}$ ,  $g =$

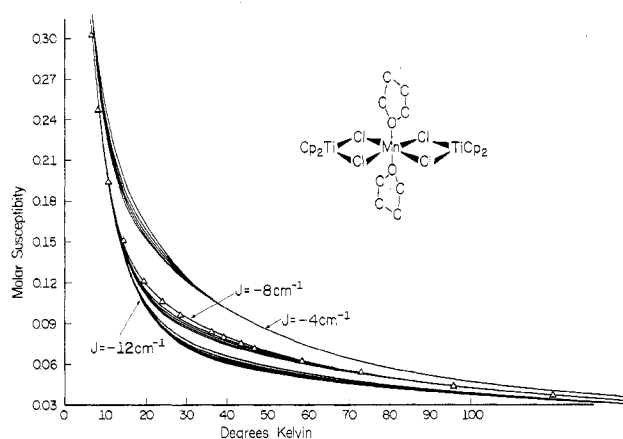


**Figure 7.** Magnetic susceptibility vs. temperature curve for  $[(C_5H_5)_2Ti]_2MnCl_4 \cdot 2OC_4H_8$ . The  $J$  value indicated for each cluster of curves is  $J_{1/2,5/2}$  and each cluster contains curves representing values of  $J_{1/2,1/2}$  of  $-8$ ,  $-4$ ,  $0$ ,  $4$ , and  $8$   $cm^{-1}$ .

**Table XIII.** Magnetic Data for  $[(C_5H_5)_2TiCl]_2MnCl_2 \cdot 2THF^a$

Temp, K	$10^2 \chi_m$ , cgsu		$\mu_{eff}/unit$ , $\mu_B$	
	Obsd	Calcd	Obsd	Calcd
295.1	1.64	1.65	6.220	6.242
231.0	2.06	2.06	6.171	6.171
196.5	2.38	2.38	6.120	6.116
160.8	2.84	2.83	6.044	6.037
120.2	3.63	3.62	5.904	5.898
95.6	4.32	4.34	5.749	5.762
73.0	5.34	5.31	5.581	5.569
58.4	6.20	6.20	5.381	5.381
46.7	7.15	7.15	5.168	5.168
43.5	7.47	7.47	5.097	5.097
39.1	7.94	7.95	4.983	4.986
36.1	8.33	8.32	4.903	4.901
28.4	9.59	9.51	4.666	4.646
24.0	10.58	10.44	4.506	4.477
19.4	12.14	11.88	4.340	4.292
14.4	15.12	10.79	4.173	4.127
10.7	19.43	19.46	4.078	4.081
8.2	24.77	25.78	4.031	4.112
6.6	30.27	32.89	3.997	4.167
5.4	36.92	41.59	3.993	4.238
4.8	41.32	47.93	3.983	4.290
4.2	46.00	56.57	3.931	4.359

<sup>a</sup>  $J_{1,2} = -8.24$   $cm^{-1}$ ,  $J_{1,3} = -8.08$   $cm^{-1}$ ,  $g = 2.00$ ,  $\Theta = 0.87$  K, and  $TIP = 260 \times 10^{-6}$  per trimetallic unit.

2.00, and  $\Theta = 0.87$  K. The experimental and calculated data from which these parameters were obtained are given in Table XIII. The TIP was set at  $260 \times 10^{-6}$  cgsu/molecule as for the compounds with a diamagnetic metal bridge since the manganese atom with its  $^6A$  ground state was expected to make a negligible contribution. In Figure 7 the  $J$  indicated for each cluster of curves is  $J_{1/2,5/2}$ , and each line within a cluster is a different value for  $J_{1/2,1/2}$  ranging from  $-8$  to  $+8$  in steps of  $4$   $cm^{-1}$ . It is apparent that the fit is very insensitive to large changes in  $J_{1/2,1/2}$  and that the final value for this parameter is probably dependent on the magnitude of  $J_{1/2,5/2}$ . While the value of  $J_{1/2,1/2}$  obtained from the fitting procedure is not unreasonable in light of the results for complexes with a diamagnetic metal bridge, it cannot be stated conclusively that interaction between the terminal titanium atoms has been detected in this case. Sinn also encountered this problem when studying copper trimetallic complexes and noted that central metal atoms with fewer unpaired electrons would form compounds whose magnetic properties would be more sensitive to small changes in the interaction parameters.<sup>9</sup> For the titanium compounds, extension of the series to include other paramagnetic central metals ( $d^2$ ,  $d^3$ , and  $d^8$ ) has not been

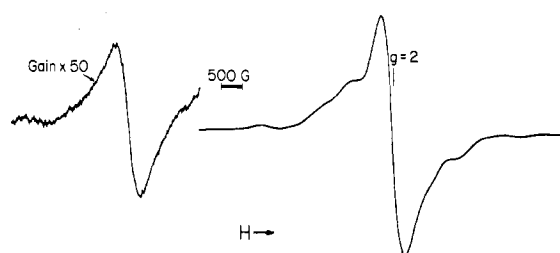


**Figure 8.** Q-Band powder EPR spectrum of  $[(C_5H_5)_2TiCl]_2MnCl_2 \cdot 2OC_4H_8$ .

successful and the synthetic problems encountered have been discussed elsewhere.<sup>13</sup>

The magnetic susceptibility of the manganese-bridged compound was simulated ignoring any zero-field splitting on the tetragonal manganese site. Figure 8, which shows a powder EPR spectrum of this complex, indicates that the manganese zero-field splitting is fairly small. A  $g$  value of 2.004 is estimated for the most intense peak in the spectrum, and the line shape appears compatible with a five-line manganese spectrum overlapping a Ti(III) feature near the center. The 1500-G separation of two of the outer manganese peaks can be used to estimate a magnitude for  $D$  of about  $0.07$   $cm^{-1}$ . Dowsing and co-workers have studied a series of tetragonal manganese(II) compounds with varying  $D$  values in the range  $0.035$ – $0.87$   $cm^{-1}$ .<sup>30</sup> Comparison of their EPR spectra with that of the titanium complex indicates the basic shape is the same for  $Mn(\gamma-pic)_4(NCS)_2$  which has a  $D$  value of  $0.035$   $cm^{-1}$  and also shows the highest intensity at  $g = 2$ . For higher values of  $D$ , the strongest line in the spectrum was found at a  $g$  of approximately 6. An attempt was made to prepare the scandium analogue of the titanium trimetallic compound by reacting  $[(\eta^5-C_5H_5)_2ScCl]_2$  with anhydrous  $MnCl_2$  in THF, but  $MnCl_2$  proved to be totally unreactive and only starting material was recovered. Synthesis of this compound would have allowed verification of the EPR spectrum of the manganese site without the complicating effects of exchange coupling or overlap from the spectrum of another paramagnetic center.

### Summary

An antiferromagnetic interaction has been observed between  $(C_5H_5)_2Ti$  groups bridged by diamagnetic, tetrahedrally coordinated zinc and beryllium halides. The magnitude of this effect has been found to be relatively unchanged by substitution of a methyl group on the cyclopentadienyl ring or perturbation of the ring–titanium–ring angle. Replacement of zinc as the bridging metal by beryllium, which does not have  $d$  orbitals available to propagate the electronic coupling, also seems to have little effect. The only substitution which altered the magnitude of the coupling was replacement of the bridging chlorine atoms by bromine atoms. The available facts indicate that the exchange pathway involves superexchange via the halides and that there is not a substantial direct overlap of metal orbitals.

The situation in the manganese-bridged compound is less clear since the larger number of unpaired electrons masks the effect of the antiferromagnetic coupling. An antiferromagnetic interaction between titanium and manganese is indicated, but inclusion of a term for titanium–titanium coupling in simulating the magnetic susceptibility could not be justified. A crystallographic determination shows tetragonal rather than tetrahedral symmetry around the manganese atom and the effect of this on the nature of the exchange pathway is not known, although it is believed that superexchange is still responsible for the observed coupling.

**Acknowledgment.** This research was supported by the National Science Foundation under Grants NSF DMR

7203026 and MPS 74-23000. We are also grateful to Professor D. N. Hendrickson and members of his group for assistance in collecting low-temperature magnetic susceptibility data.

**Registry No.**  $[(\eta^5\text{-C}_5\text{H}_5)_2\text{TiCl}]_2\text{MnCl}_2 \cdot 2(\text{OC}_4\text{H}_8)$ , 55799-99-0;  $(\eta^5\text{-C}_5\text{H}_5)_2\text{TiCl}_2$ , 1271-19-8;  $(\eta^5\text{-C}_5\text{H}_5)_2\text{VCl}_2$ , 12083-48-6;  $[(\eta^5\text{-C}_5\text{H}_5)_2\text{TiCl}]_2\text{ZnCl}_2 \cdot 2\text{C}_6\text{H}_6$ , 54040-41-4;  $[(\eta^5\text{-C}_5\text{H}_5)_2\text{TiBr}]_2\text{ZnBr}_2$ , 54004-69-2;  $[(\eta^5\text{-C}_5\text{H}_5)_2\text{TiCl}]_2\text{BeCl}_2$ , 54004-68-1;  $[(\text{CH}_3\text{C}_5\text{H}_4)_2\text{Ti}]_2\text{ZnCl}_4$ , 54064-96-9;  $[(\text{CH}_3)_2\text{Si}(\text{C}_5\text{H}_4)_2\text{Ti}]_2\text{ZnCl}_4$ , 55800-01-6.

**Supplementary Material Available:** Figure 9, showing temperature dependence of magnetic susceptibility and effective moment per Ti for  $[(\eta^5\text{-CH}_3\text{C}_5\text{H}_4)_2\text{TiCl}]_2\text{ZnCl}_2$ , Table VII, listing observed and calculated structure factors for  $[(\eta^5\text{-C}_5\text{H}_5)_2\text{TiCl}]_2\text{MnCl}_2 \cdot 2\text{OC}_4\text{H}_8$ , and Tables VIII–XII, giving magnetic data for  $[(\eta^5\text{-C}_5\text{H}_5)_2\text{TiCl}]_2\text{ZnCl}_2 \cdot 2\text{C}_6\text{H}_6$ ,  $[(\eta^5\text{-C}_5\text{H}_5)_2\text{TiBr}]_2\text{ZnBr}_2 \cdot 2\text{C}_6\text{H}_6$ ,  $[(\eta^5\text{-C}_5\text{H}_5)_2\text{TiCl}]_2\text{BeCl}_2 \cdot 2\text{C}_6\text{H}_6$ ,  $[(\eta^5\text{-CH}_3\text{C}_5\text{H}_4)_2\text{Ti}]_2\text{ZnCl}_2$ , and  $[(\text{CH}_3)_2\text{Si}(\eta^5\text{-C}_5\text{H}_4)_2\text{Ti}]_2\text{ZnCl}_2$  (24 pages). Ordering information is given on any current masthead page.

## References and Notes

- (1) L. V. Interrante, Ed., *ACS Symp. Ser.*, No. 5 (1974).
- (2) D. J. Hodgson, *Prog. Inorg. Chem.*, **19**, 173 (1975).
- (3) M. D. Glick and R. L. Lintvedt, *Prog. Inorg. Chem.*, **21**, 233 (1976).
- (4) B. N. Figgis and G. Robertson, *Nature (London)*, **205**, 694 (1965).
- (5) J. Wucher and H. M. Gijssman, *Physica (Utrecht)*, **20**, 361 (1954).
- (6) J. Wucher and J. D. Wasscher, *Physica (Utrecht)*, **20**, 721 (1954).
- (7) A. Earnshaw, B. N. Figgis, and J. Lewis, *J. Chem. Soc. A*, 1656 (1966).

- (8) R. W. Adams, C. G. Barraclough, R. L. Martin, and G. Winter, *Inorg. Chem.*, **5**, 346 (1966).
- (9) S. J. Gruber, C. M. Harris, and E. Sinn, *J. Chem. Phys.*, **49**, 2183 (1968).
- (10) A. P. Ginsberg, R. L. Martin, and R. C. Sherwood, *Chem. Commun.*, 856 (1967).
- (11) A. P. Ginsberg, R. L. Martin, and R. C. Sherwood, *Inorg. Chem.*, **7**, 932 (1968).
- (12) R. Jungst, D. Sekutowski, and G. Stucky, *J. Am. Chem. Soc.*, **96**, 8108 (1974).
- (13) D. G. Sekutowski and G. D. Stucky, *Inorg. Chem.*, **14**, 2192 (1975).
- (14) D. T. Cromer and J. T. Waber, *Acta Crystallogr.*, **18**, 104 (1965).
- (15) R. F. Stewart, E. R. Davidson, and W. T. Simpson, *J. Chem. Phys.*, **42**, 3175 (1965).
- (16) D. T. Cromer and D. Liberman, *J. Chem. Phys.*, **53**, 1891 (1970).
- (17) D. G. Sekutowski and G. D. Stucky, *J. Am. Chem. Soc.*, **98**, 1376 (1976).
- (18) E. Sinn, *Coord. Chem. Rev.*, **5**, 313 (1970).
- (19) R. D. W. Kemmitt in "Comprehensive Inorganic Chemistry", J. C. Bailar, H. J. Emelius, R. Nyholm, and A. F. Trotman-Dickenson, Ed., Pergamon Press, London, 1973, pp 790–793, and references therein.
- (20) C. J. Ballhausen and J. P. Dahl, *Acta Chem. Scand.*, **15**, 1333 (1961).
- (21) C. J. Ballhausen and J. P. Dahl, *Acta Chem. Scand.*, **15**, 1333 (1961).
- (22) N. W. Alcock, *J. Chem. Soc. A*, 2001 (1967).
- (23) J. C. Green, M. L. H. Green, and C. K. Prout, *J. Chem. Soc., Chem. Commun.*, 421 (1972).
- (24) A. Nakamura and S. Ottuka, *J. Am. Chem. Soc.*, **95**, 5091 (1973).
- (25) J. L. Petersen and L. F. Dahl, *J. Am. Chem. Soc.*, **97**, 6422 (1975).
- (26) J. L. Petersen and L. F. Dahl, *J. Am. Chem. Soc.*, **96**, 2248 (1974).
- (27) J. L. Petersen and L. F. Dahl, *J. Am. Chem. Soc.*, **97**, 6416 (1975).
- (28) J. L. Petersen, D. L. Lichtenberger, R. F. Fenske, and L. F. Dahl, *J. Am. Chem. Soc.*, **97**, 6433 (1975).
- (29) R. Jungst, D. Sekutowski, J. Davis, M. Luly, and G. Stucky, *Inorg. Chem.*, **16**, 1645 (1977).
- (30) R. L. Martin, *New Pathways Inorg. Chem.*, 175 (1968).
- (31) R. D. Dowsing, J. F. Gibson, M. Goodgame, and P. J. Hayward, *J. Chem. Soc. A*, 187 (1969).

Contribution from the Department of Physical and Inorganic Chemistry, University of Adelaide, Adelaide, South Australia 5001, Australia

## Proton Magnetic Resonance Study of Ligand Exchange on Tetrakis(hexamethylphosphoramidate)dioxouranium(VI)

GEOFFREY J. HONAN, STEPHEN F. LINCOLN,\* and EVAN H. WILLIAMS

Received November 23, 1977

$^1\text{H}$  NMR studies show the rate law for hexamethylphosphoramidate (HMPA) exchange on  $\text{UO}_2(\text{HMPA})_4^{2+}$  to be rate =  $4(k_1 + k_2[\text{HMPA}])[\text{UO}_2(\text{HMPA})_4^{2+}]$  in  $\text{CD}_2\text{Cl}_2$  diluent, where  $k_1(273\text{ K}) = 12.5 \pm 1.1\text{ s}^{-1}$ ,  $\Delta H^\ddagger = 14.0 \pm 3.0\text{ kJ mol}^{-1}$ , and  $\Delta S^\ddagger = -172 \pm 11\text{ J K}^{-1}\text{ mol}^{-1}$  and  $k_2(273\text{ K}) = 173 \pm 15\text{ mol}^{-1}\text{ dm}^3\text{ s}^{-1}$ ,  $\Delta H^\ddagger = 22.2 \pm 3.0\text{ kJ mol}^{-1}$ , and  $\Delta S^\ddagger = -120 \pm 9\text{ J K}^{-1}\text{ mol}^{-1}$ . This two-term rate law contrasts with the first-order rate law observed for the exchange of oxygen donor ligands L in some  $\text{UO}_2\text{L}_5^{2+}$  species, and the origins of the two different rate laws are discussed in terms of dissociative and associative exchange mechanisms.

### Introduction

In the solid state the presence of four, five, and six oxygen donor ligand atoms in the equatorial plane of dioxouranium(VI) species is well established.<sup>1–3</sup> These ground-state occupancies might indicate the possibilities of similar variations in transition-state equatorial occupancies but the monodentate oxygen donor ligand (L) species  $\text{UO}_2\text{L}_5^{2+}$  so far investigated in several noncoordinating solvents (L = dimethylacetamide (DMA),<sup>4</sup> dimethyl methylphosphonate (DMMP),<sup>5</sup> trimethyl phosphate (TMP),<sup>6</sup> triethyl phosphate (TEP),<sup>6</sup> tetramethylurea (TMU),<sup>7</sup> and dimethyl sulfoxide ( $\text{Me}_2\text{SO}$ )<sup>8</sup>) have all exhibited a first-order ligand exchange rate law consistent with a dissociative (D) or dissociative interchange ( $\text{I}_\text{D}$ ) mechanism and a six-coordinate (including the axial oxo ligands) transition state or reactive intermediate. Consequently, ligand exchange studies on  $\text{UO}_2(\text{HMPA})_4^{2+}$  (where HMPA is hexamethylphosphoramidate) have been carried out in order to determine the effect of the reduced equatorial plane occupancy of the ground state of this species on the ligand exchange mechanism.

### Experimental Section

Dioxotetrakis(hexamethylphosphoramidate)uranium(VI) perchlorate was prepared under dry nitrogen by refluxing hydrated dioxo-

uranium(VI) perchlorate (G. Frederick Smith) (2.5 g) with triethyl orthoformate (10 g) at 320–330 K for 1 h.<sup>9,10</sup> Dry HMPA (Koch-Light) (3.75 g) was then added at room temperature, and the resultant pale yellow crystals were filtered off, washed with dry ether, and pumped down on a vacuum line for several hours. At all times exposure of the product to light was kept to a minimum to minimize the possibility of photochemically induced redox processes.<sup>11</sup> Anal. Calcd for  $[\text{UO}_2(\text{HMPA})_4](\text{ClO}_4)_2$ : C, 24.31; H, 6.12; N, 14.18; P, 10.45; U, 20.07. Found: C, 24.16; H, 6.13; N, 14.54; P, 10.5; U, 19.87. The yield was 96%. Analyses for U as  $\text{UO}_2^{2+}$  were made with an ion-exchange technique,<sup>12</sup> and C, H, and N analyses were carried out by the Australian Microanalytical Service, Melbourne. No explosion hazard was encountered with  $[\text{UO}_2(\text{HMPA})_4](\text{ClO}_4)_2$ , but it should be noted that such perchlorate salts are potentially explosive.

Solutions of  $[\text{UO}_2(\text{HMPA})_4](\text{ClO}_4)_2$  and HMPA in  $\text{CD}_2\text{Cl}_2$  diluent (CEA 99.4%) were prepared under dry nitrogen in 5-cm<sup>3</sup> volumetric flasks. Each solution was transferred to a 5 mm o.d. NMR tube and was degassed on a vacuum line prior to sealing under vacuum not more than 1 h before commencement of the NMR experiment. The redistilled HMPA and  $\text{CD}_2\text{Cl}_2$  were thoroughly dried over Linde 4A molecular sieves prior to use.

Proton NMR spectra were run at 90 MHz on a Bruker HX90E spectrometer in PFP mode using a deuterium lock. Depending upon the concentration of the sample, up to ten spectra were computer (Nicolet BNC-12) averaged, and these spectra were then digitized